Some numerical strategies to be improved for controlled fusion designed.

B. Nkonga,
with
R. Abgrall, B. Braconnier, R. Butel, A. Bourgeade, G. Huysmans, P.H. Maire, V. Tikhonchuk, ...

JAD Univ. Nice/INRIA Sophia-Antipolis

1ères journées du GDR Calcul : 9-10 novembre 2009

Inertial Confinement Fusion : Compression Ignition

- Ignition by lasers compression

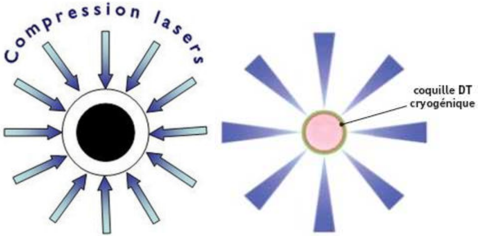

- Interfaces flow
- Large ratio computational domain change.

Needs : Lagrangian Hydrodynamics Scheme...

- Ignition by X-rays compression

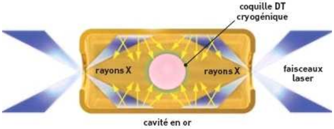

Needs : Compute Focusing Beams interactions...

Inertial Confinement Fusion : Fast laser ignition

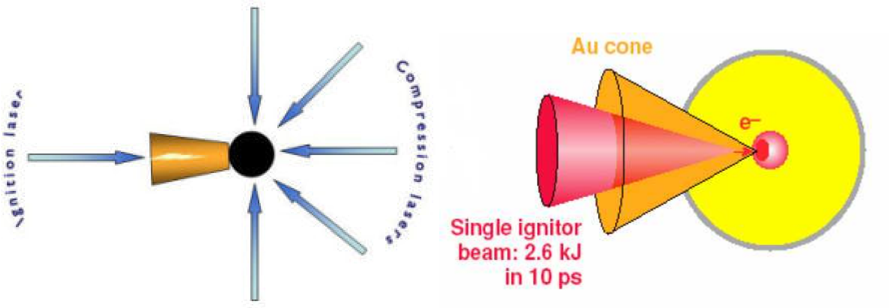

Need : Nonlinear laser/plasmas model, non-local Transport...

Tokamak Plasma : Avoid large scale instabilities.

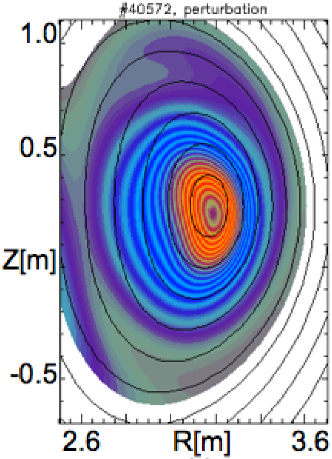

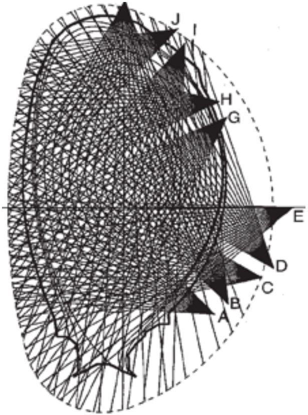

Tomographic reconstruction of X-ray emission. JET SXR cameras (1998).

Tokamak Plasma : Kink instability (MHD, Jorek).

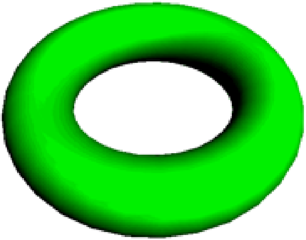

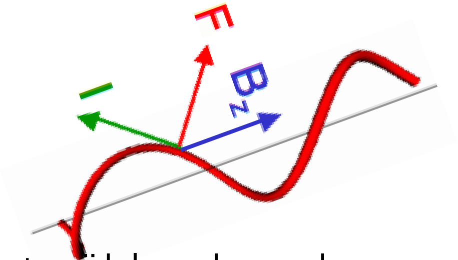

n toroïdal mode number
m poloïdal mode number

$$q = \frac{m=3}{n=1}$$

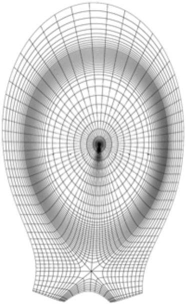

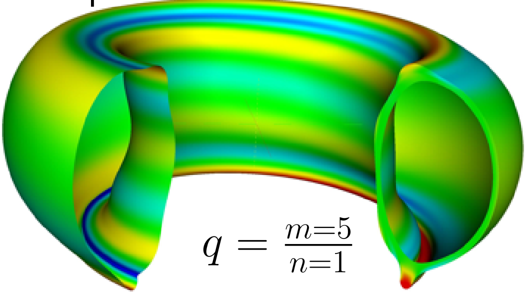

$$q = \frac{m=5}{n=1}$$

Laser focusing (ICF): Huygens-Fresnel Theorem.

$\simeq 30$ Laser Quads

$4(40cm \times 40cm)$.

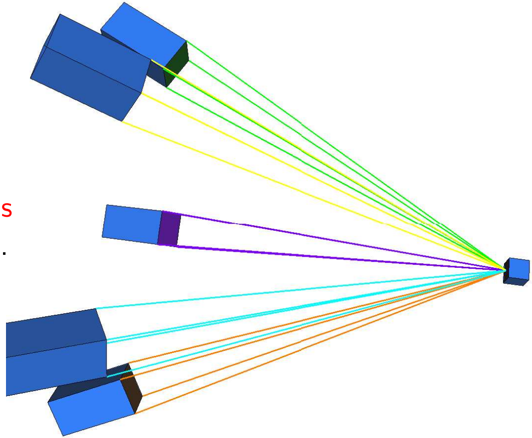

Focal spot

$\simeq 1mm \times 1mm$

$$\boldsymbol{E}(t,\boldsymbol{x}) = \int_{\mathbb{R}^2} d\boldsymbol{\theta} \int_{\mathbb{R}} d\omega \, \hat{\mathcal{E}}(\boldsymbol{\theta},\omega) \, \exp\left[\imath\left(\boldsymbol{\theta}\cdot\boldsymbol{\xi}(\boldsymbol{x}) + k_0 n_0(\boldsymbol{x}) - \omega t\right)\right]$$

Focusing Laser : Approximations and Computations.

$$\boldsymbol{E}(\boldsymbol{x},t)=\sum_{\ell=1}^{N_\ell}\sum_{m=1}^{N_w}\sum_{i=1}^{Nk_x}\sum_{j=1}^{Nk_y}\mathcal{E}_{\ell,i,j,m}\mathcal{G}_{\ell,h}(t,\boldsymbol{x},\omega_m,\boldsymbol{\theta}_{ij})e^{\imath\Phi_{l,i,j,m}}e^{\imath\omega_m\left(t-\frac{n_\ell(\boldsymbol{x})}{c}\right)}$$

where $\quad \Phi_{l,i,j,m}=\boldsymbol{\beta}_\ell(\boldsymbol{x})\cdot\boldsymbol{k}_\ell(\boldsymbol{\theta}_{ij},\omega_m)+\dfrac{\omega_m n_\ell(\boldsymbol{x})}{c}$

$$\boldsymbol{k}_\ell(\boldsymbol{\theta},\omega)=k_{0,\ell}(\boldsymbol{\theta},\omega)\boldsymbol{n}_{0,\ell}+\theta_{1,\ell}\boldsymbol{n}_{1,\ell}+\theta_{2,\ell}\boldsymbol{n}_{2,\ell}$$

$$\boldsymbol{\beta}_\ell(\boldsymbol{x})=\boldsymbol{x}-\boldsymbol{x}_\ell=n_\ell(\boldsymbol{x})\boldsymbol{n}_{0,\ell}+\xi_{1,\ell}(\boldsymbol{x})\boldsymbol{n}_{1,\ell}+\xi_{2,\ell}(\boldsymbol{x})\boldsymbol{n}_{2,\ell}$$

Given $\mathcal{E}_{\ell,i,j,m}$
$N_l=30$ quads
Quad $\simeq 1.2m\times 1.2m$

$\boldsymbol{E}(\boldsymbol{x},t)$ to be computed with the resolution :
$Nf_x\times Nf_y\times Nf_t$
Focal spot : $1.2mm\times 1.2mm.$

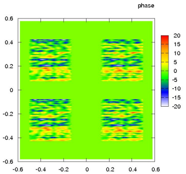

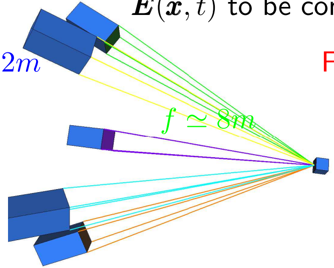

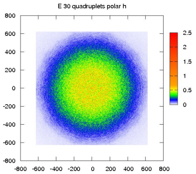

Focusing Laser Beams : CPU Consuming

Mega Joule Laser (Bordeaux) : Input and Operations

$$N_w \simeq 10^3, \quad Nk_x \simeq Nk_y \simeq 10^3 \quad N_\ell \simeq 30\text{quads}$$

$$\text{Total of Floating Operations } = \text{Flop} \simeq 3 \times 10^{10} \times \mathcal{R}_f$$

$\mathcal{R}_f = Nf_x \times Nf_y \times Nf_t$ `is the focal spot resolution`

CPU Time for $\mathcal{R}_f = 2048 \times 2048 \times 1000 \simeq 4 \times 10^9$

Flop $\simeq 10^{20} = 10^8$Tera $\Longrightarrow$ $\underline{28 \times 10^3 \text{ H with a Tera computer}}$ $\equiv$ 3 years

Parallel Computing unavoidable !

Need of mathematical approximations!

Stationary phase approximation : asymptotic of oscillatory integrals

Focusing Laser Beams : Parallel strategy (simple)

- Scatter the Flop:

$$\boldsymbol{E}(\boldsymbol{x},t,\mathtt{me}) = \sum_{\ell} \sum_{m_1(\mathtt{me})}^{m_N(\mathtt{me})} \sum_{i_1(\mathtt{me})}^{iN(\mathtt{me})} \sum_{j_1(\mathtt{me})}^{j_N(\mathtt{me})} \color{blue}{\mathcal{E}_{\ell,i,j,m}}\color{green}{\mathcal{G}_{\ell,h}}\color{black}{e^{\imath\Phi_{l,i,j,m}}e^{\imath\omega_m\tau}}$$

- Gather the solution :

$$\boldsymbol{E}(\boldsymbol{x},t) = \sum_{\mathtt{me}=0}^{N_p-1}\!\!\oplus\, \boldsymbol{E}(\boldsymbol{x},t,\mathtt{me})$$

FFTW + MPI

Focusing Laser Beams : Computed focal spot and zoom.

$\|\boldsymbol{E}(\boldsymbol{x},t)\|$

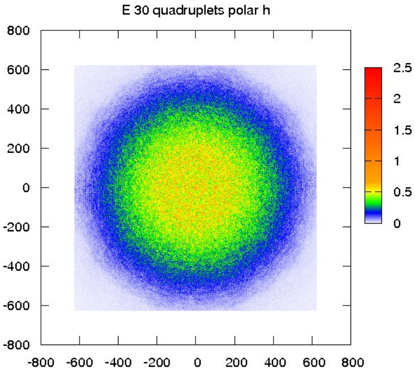

$\|\boldsymbol{E}(\boldsymbol{x},t)\|$

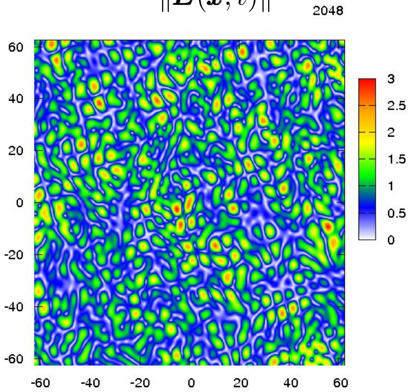

21H CPU with 1936 cores : 30 quads = 120 (40cm x 40cm)

Nodes : 4 Intel®Itanium® II, Dual-Core, 1.6 Ghz, 128 Go

$N_w = Nf_t = 1, \quad Nk_x = Nk_y = 2048$ and $Nf_x = Nf_y = 2048$

From the focal spot to Lagrangian Hydrodynamics

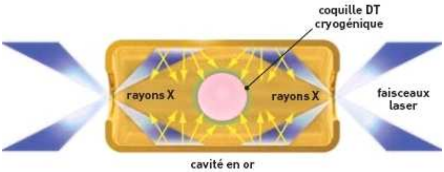

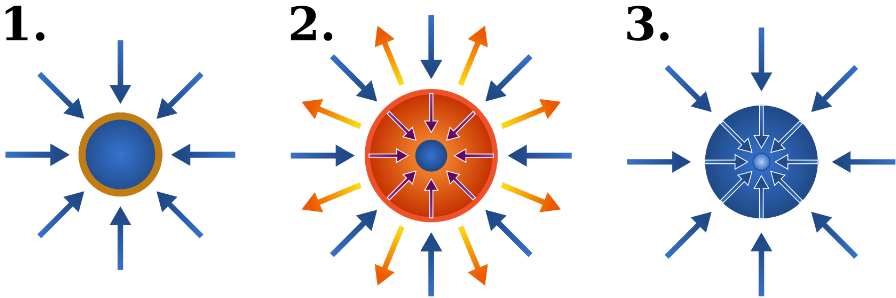

Weak formulation of Conservation Law

Integral form of in arbitrary coordinates

$$\left\{\begin{array}{lcl} \dfrac{d}{dt}\displaystyle\int_{\mathcal{C}(t)} \rho \, d\boldsymbol{x} + \int_{\partial\mathcal{C}(t)} \rho \,(\boldsymbol{u}-\boldsymbol{\kappa})\cdot\boldsymbol{n}\, dS & = & 0, \\ \dfrac{d}{dt}\displaystyle\int_{\mathcal{C}(t)} \rho\boldsymbol{u} \, d\boldsymbol{x} + \int_{\partial\mathcal{C}(t)} \rho\boldsymbol{u} \,(\boldsymbol{u}-\boldsymbol{\kappa})\cdot\boldsymbol{n}\, dS & = & -\displaystyle\int_{\partial\mathcal{C}(t)} p\boldsymbol{n}\, dS, \\ \dfrac{d}{dt}\displaystyle\int_{\mathcal{C}(t)} \rho\mathbf{e} \, d\boldsymbol{x} + \int_{\partial\mathcal{C}(t)} \rho\mathbf{e} \,(\boldsymbol{u}-\boldsymbol{\kappa})\cdot\boldsymbol{n}\, dS & = & -\displaystyle\int_{\partial\mathcal{C}(t)} p\boldsymbol{u}\cdot\boldsymbol{n}\, dS. \end{array}\right.$$

Lagrangian controle volume : $\boldsymbol{\kappa} = \boldsymbol{u}$ on $\partial\mathcal{C}(t)$

- $\tilde{m}_C \dfrac{d}{dt}\tilde{\boldsymbol{u}}_C = -\displaystyle\int_{\partial\mathcal{C}_C(t)} p\boldsymbol{n}\, dS,$
- $\tilde{m}_C \dfrac{d}{dt}\tilde{e}_C = -\displaystyle\int_{\partial\mathcal{C}_C(t)} p\boldsymbol{\kappa}\cdot\boldsymbol{n}\, dS.$

where

- $\dfrac{d}{dt}\tilde{m}_C = 0,$

Coupling between averaged(mesh scale) and subscale states.

Multiscale formulation and approximation

Mesh scale equations

- $\tilde{m}_C \frac{d}{dt}\tilde{\boldsymbol{u}}_C = -\int_{\partial\mathcal{C}_C(t)} p\boldsymbol{n}\, dS,$
- $\tilde{m}_C \frac{d}{dt}\tilde{e}_C = -\int_{\partial\mathcal{C}_C(t)} p\boldsymbol{\kappa}\cdot\boldsymbol{n}\, dS.$

where

- $\frac{d}{dt}\tilde{m}_C = 0,$

sub-scale $\mathcal{K}^\epsilon_{j,C} \subset \mathcal{C}_C$ and $\mathcal{K}^\epsilon_{j,C} \subset \mathcal{K}^\epsilon_j$ :: $\epsilon \mapsto 0$

$$\frac{d}{dt}\int_{\mathcal{K}^\epsilon_j(t)} \rho\boldsymbol{\kappa}\, d\boldsymbol{x} = -\int_{\partial\mathcal{K}^\epsilon_j(t)} p\boldsymbol{n}\, dS, \qquad |\mathcal{K}^\epsilon_j| \simeq O(\epsilon)$$

$$\frac{d}{dt}\int_{\mathcal{K}^\epsilon_{j,C}(t)} \rho\boldsymbol{\kappa}\, d\boldsymbol{x} = -\int_{\partial\mathcal{K}^\epsilon_{j,C}(t)} p\boldsymbol{n}\, dS, \qquad |\mathcal{K}^\epsilon_{j,C}| \simeq O(\epsilon)$$

Subscale Riemann Problem to compute $p^*_{C,\ell,j}$ and $\boldsymbol{\kappa}_j$

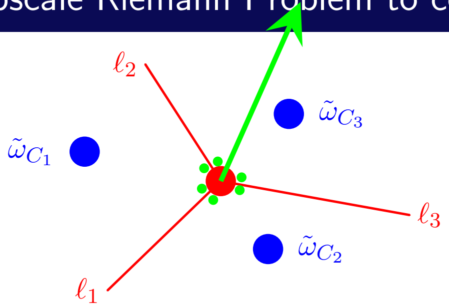

Half Riemann Solver for $\boldsymbol{\kappa}_j$ fixed: Godunov-type method

$$p^*_{C,\ell,j} = p^*_\ell\left(\tilde{\omega}_C, \boldsymbol{\kappa}_j\right) = p_C + Z_{C,j}\left(\tilde{\boldsymbol{u}}_C - \boldsymbol{\kappa}_j\right) \cdot \frac{\boldsymbol{m}_{C,\ell,j}}{\|\boldsymbol{m}_{C,\ell,j}\|}$$

Subscale compatibility: The local system can be nonlinear: $\hookrightarrow \boldsymbol{\kappa}_j$

$$\sum_{\ell \in \vartheta(j)} r_\ell (p^*_{C_1,\ell,j} - p^*_{C_2,\ell,j}) \boldsymbol{n}_{C_1,\ell} = 0$$

Subscale Riemann Problem to compute $p^*_{C,\ell,j}$ and $\boldsymbol{\kappa}_j$

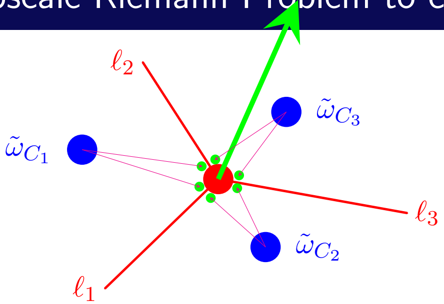

Half Riemann Solver for $\boldsymbol{\kappa}_j$ fixed: Godunov-type method

$$p^*_{C,\ell,j} = p^*_\ell\left(\tilde{\omega}_C, \boldsymbol{\kappa}_j\right) = p_C + Z_{C,j}\left(\tilde{\boldsymbol{u}}_C - \boldsymbol{\kappa}_j\right) \cdot \frac{\boldsymbol{m}_{C,\ell,j}}{\|\boldsymbol{m}_{C,\ell,j}\|}$$

Subscale compatibility: The local system can be nonlinear: $\hookrightarrow \boldsymbol{\kappa}_j$

$$\sum_{\ell \in \vartheta(j)} r_\ell (p^*_{C_1,\ell,j} - p^*_{C_2,\ell,j}) \boldsymbol{n}_{C_1,\ell} = 0$$

Numerical Scheme : Linear mapping for $\psi_{\ell,j}(\xi)$

$$p_\ell^*\left(\tilde{\omega}_C, \boldsymbol{\kappa}_j\right) = p_C + Z_{C,j}\left(\tilde{\boldsymbol{u}}_C - \boldsymbol{\kappa}_j\right)\cdot \boldsymbol{m}_{C,\ell,j}$$

Explicit scheme : $\left[\mathcal{A}_j\left(\tilde{\omega}_*^n,\ \boldsymbol{\kappa}_*^n\right)\right]\boldsymbol{\kappa}_j^* = \boldsymbol{g}_j\left(\tilde{\omega}_*^n,\ \boldsymbol{\kappa}_*^n\right) \longrightarrow \boldsymbol{x}^{n+\theta}$

$$\boldsymbol{\kappa}_\ell(\boldsymbol{x}) = \sum \varphi_{\ell,j}(\mathbf{x})\boldsymbol{\kappa}_j^*, \qquad p_{C,\ell}(\boldsymbol{x}) = \sum \psi_{\ell,j}(\mathbf{x}) p_\ell^*\left(\tilde{\omega}_C^n, \boldsymbol{\kappa}_j^*\right)$$

$$\tilde{m}_C \frac{d}{dt}\tilde{\boldsymbol{u}}_C = -\sum_{\ell\in\partial C}\int_\ell p_{C,\ell}(\boldsymbol{x})\boldsymbol{n}(\boldsymbol{\kappa}_*^n)\ d\ell,$$

$$\tilde{m}_C \frac{d}{dt}\tilde{e}_C = -\sum_{\ell\in\partial C}\int_\ell p_{C,\ell}(\boldsymbol{x})\boldsymbol{\kappa}_\ell(\boldsymbol{x})\cdot \boldsymbol{n}(\boldsymbol{\kappa}_*^n)\ d\ell.$$

Orthogonality constraint for interpolation gives

$$\psi_{\ell,j}(\xi) = (d+1)\varphi_{\ell,j}(\xi) - 1$$

and

$$\int_\ell \psi_{\ell,i}\varphi_{\ell,j} d\ell = \frac{\|\ell\|}{d}\delta_{i,j}$$

Therefore we have analitical formula for the right hand side to compute
$\hookrightarrow \boldsymbol{u}^{n+\theta}, e^{n+\theta}, \rho^{n+\theta}, p^{n+\theta} \hookrightarrow \tilde{\omega}^{n+\theta}$

Saltzman problem

Computational domain $(x, y) \in [0, 1] \times [0, 0.1]$ with $(n_x, n_y) = (100, 10)$ skewed by the map

$$x_{\mathsf{sk}} = x + (0.1 - y)\sin(\pi x), \quad y_{\mathsf{sk}} = y.$$

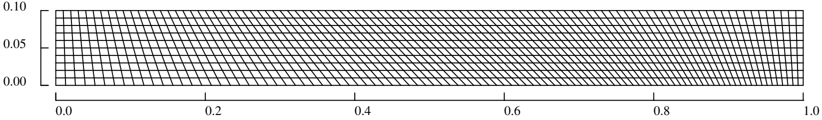

Initial conditions: $(\rho^0, P^0, \boldsymbol{U}^0) = (1, 10^{-6}, 0)$

Materials: gamma law gas with $(\gamma = 5/3)$

Boundary conditions: inflow velocity $U^{\star} = 1$ at $x = 0$.

Saltzman problem : Density at $t = 0.6$

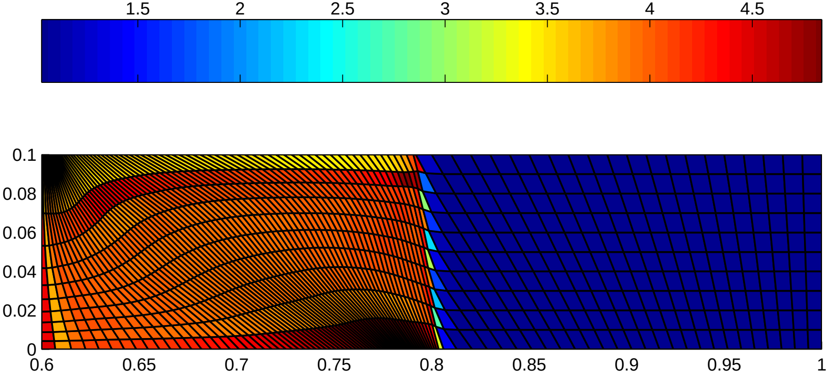

Cylindrical Noh Problem: non-conformal, 2250 cells

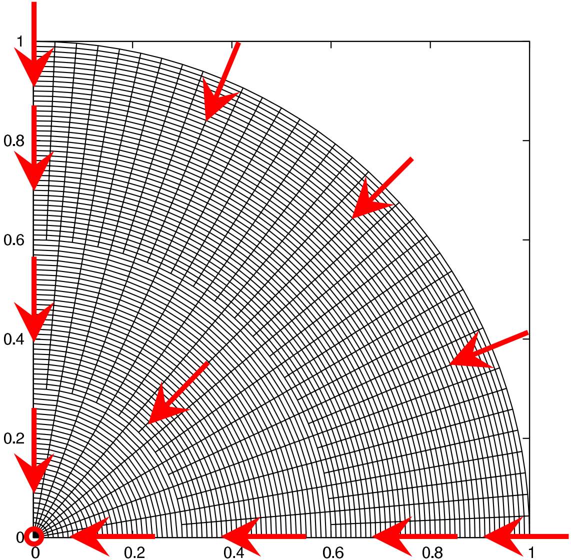

Sedov-Taylor blast wave: 31×31 Cartesian grid

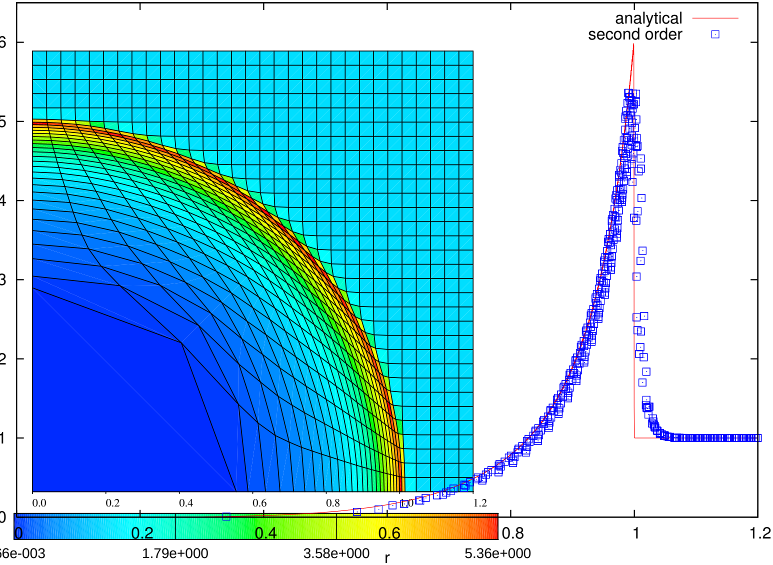

Density map (left) and density in all the cells (right) at $t = 1$.

Sedov-Taylor blast wave: 3D hexahedra mesh

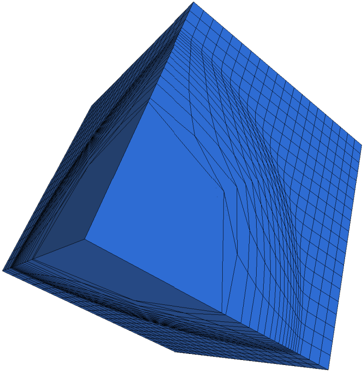

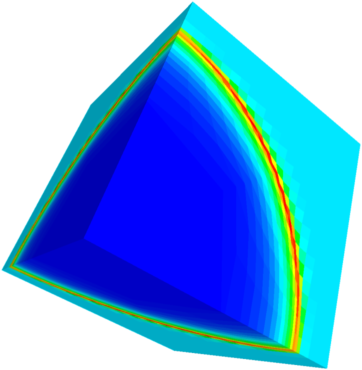

- Initial high pressure in only one cell.
- Symmetry boundary conditions

Multifluid Hydrodynamic 3D : 8×10^6 unknowns

$$\omega = (\alpha, \rho_1, \rho_2, \rho \boldsymbol{u}, E)^T$$

Implicit Low mach scheme, Surface tension, Gravity.
1.3×10^6 Cells, Time Steps = 14 610, Final Physical Time = 3.59s,
RAM used = 1.35Go/Core $\simeq$ 11 Go, CPU = 12 days$\times$ 8Pe

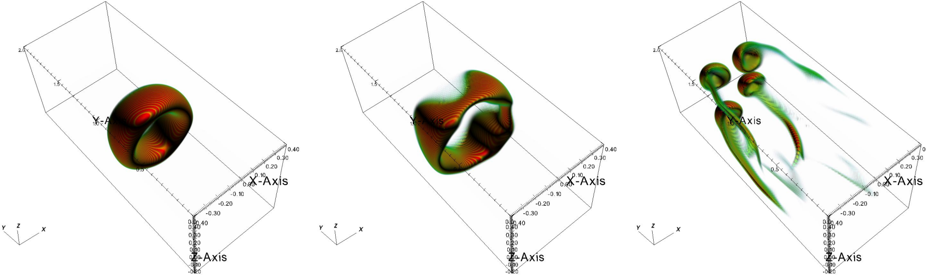

Pe : 2x3GHz Quad-core Intel Xeon
RAM: 16 Go 667MHz DDR2 FB-DIMM

Multifluid Hydrodynamic 3D : 8×10^6 unknowns

Explicit scheme : CFL 0.9

$$\frac{T_{phys}}{T_{cpu}} \simeq 1.7 \times 10^{-4}$$

$$\text{RAM used} = 0.45\text{Go}/\text{Core} \simeq 3.6\text{Go}$$

Implicit scheme : CFL 40 (GS Relaxations $\leq$ 25, $\varepsilon = 10^{-5}$)

$$\frac{T_{phys}}{T_{cpu}} \simeq 15 \times 10^{-4}$$

$$\text{RAM used} = 1.35\text{Go}/\text{Core} \simeq 11 \text{ Go}$$

$$\mathcal{E}_{cpu} = \frac{15}{1.7} \simeq 9 \qquad \mathcal{E}_{ram} = \frac{11}{3.6} \simeq 3$$

From Lagrangian Hydrodynamics to Nonlinear Laser/plasmas interaction

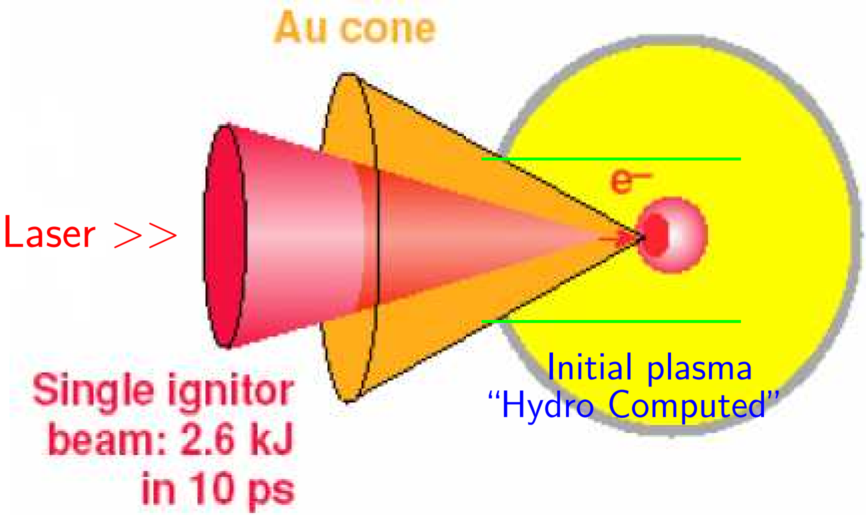

Laser/plasma interaction : Physical Model

- Paraxial approximation:

$$\frac{2\imath\omega_0}{c^2}\partial_t \mathbf{E} + 2\imath k_0 \partial_z \mathbf{E} + \left(\imath\partial_z k_0 - \frac{\omega_0^2}{c^2}\frac{n_e - n_{e0}}{n_c} + \imath\frac{\nu_{ei}\omega_0}{c^2}\frac{n_{e0}}{n_c}\right)\mathbf{E} + \left(\frac{2\nabla^2}{1+\sqrt{1+\nabla^2/k_0^2}}\right)\mathbf{E} = 0.$$

Nonlinear nonlocal laser/plasma interaction

$$\begin{aligned}
\partial_t\rho + \mathbf{u}\cdot\nabla\rho &= -\rho\nabla\cdot\mathbf{u} & & ,\\
\partial_t\mathbf{u} + \mathbf{u}\cdot\nabla\mathbf{u} &= -\frac{1}{\rho}\nabla p & -\frac{Z\nabla\left(\|\mathbf{E}\|^2\right)}{2cn_c m_i} & +\frac{1}{\rho}\nabla\cdot(\eta\nabla\mathbf{u}),\\
\partial_t T_e + \mathbf{u}\cdot\nabla T_e &= -\frac{p_e}{\rho}\nabla\cdot\mathbf{u} & +\frac{\nu_{ei}\Gamma_e}{n_c c}\|\mathbf{E}\|^2 & +\frac{\Gamma_e}{n_e}\nabla\cdot(\kappa_e\nabla T_e),\\
\partial_t T_i + \mathbf{u}\cdot\nabla T_i &= -\frac{p_i}{\rho}\nabla\cdot\mathbf{u} & & +\frac{\Gamma_i}{n_i}\nabla\cdot(\kappa_i\nabla T_i).\\
\beta_z\partial_z\mathbf{E} &= -\beta_t\partial_t\mathbf{E} & -\mathcal{S}(\rho)\mathbf{E} & -\mathcal{L}(\nabla)\mathbf{E}
\end{aligned}$$

Numerical Approximation : $\mathbf{W} = (\rho, \mathbf{u}, T_e, T_i)^T$

$$\begin{cases} \partial_t \mathbf{W} + \mathcal{A}(\mathbf{W})\nabla_{x,y}\mathbf{W} & = & \mathcal{P}(\mathbf{W}, \mathbf{E}) & + \mathcal{N}(\mathbf{W}), \\ \beta_z \partial_z \mathbf{E} & = & -\mathcal{S}(\mathbf{W})\mathbf{E} & -\mathcal{L}(\nabla_{x,y})\,\mathbf{E} \end{cases}$$

Given $\underline{\mathbf{E}^n(z=0),\ \mathbf{W}^{n-\frac{1}{2}}\left(z + \frac{\delta z}{2}\right)}$ and set $\mathcal{M}^{n-\frac{1}{2}}_{z+\frac{\delta z}{2}} = \mathcal{S}^{n-\frac{1}{2}}_{z+\frac{\delta z}{2}} + \mathcal{L}(\nabla_{x,y})$

1. FFTW & θ-scheme + MPI $\Longrightarrow \mathbf{E}^n(z + \delta z)$

$$\left[\beta_z + \delta z \theta \mathcal{M}^{n-\frac{1}{2}}_{z+\frac{\delta z}{2}}\right] \mathbf{E}^n(z+\delta z) = \left[\beta_z - \delta z (1-\theta) \mathcal{M}^{n-\frac{1}{2}}_{z+\frac{\delta z}{2}}\right] \mathbf{E}^n(z)$$

2. FV Second order accurate + MPI $\Longrightarrow \mathbf{W}^{(1)}_{i,j}\left(z + \frac{\delta z}{2}\right)$

$$\mathbf{W}^{(1)}_{i,j} = \mathbf{W}^{n-\frac{1}{2}}_{i,j} + \frac{\delta t}{a_{i,j}}\left[-\Phi^{n-\frac{1}{2}}_{i,j} + a_{i,j}\mathcal{P}^{n-\frac{1}{2}}_{i,j}\left(\frac{\mathbf{E}^n(z+\delta z) + \mathbf{E}^n(z)}{2}\right)\right]$$

3. FFTW & θ-scheme + MPI $\Longrightarrow \mathbf{W}^{n+\frac{1}{2}}\left(z + \frac{\delta z}{2}\right)$

$$\mathbf{W}^{n+\frac{1}{2}}_{i,j} - \delta t \theta \mathcal{N}_{i,j}\left(\mathbf{W}^{n+\frac{1}{2}}\right) = \mathbf{W}^{(1)}_{i,j} + \delta t (1-\theta)\mathcal{N}_{i,j}\left(\mathbf{W}^{(1)}\right)$$

Validation by a proton diagnostic.

- Incoming Electric field : $I(t, \mathbf{r}) = I_{max} \exp\left(-\frac{\mathbf{2r}}{W_0^2} - \frac{t^2}{t_0^2}\right).$

  $I_{max} = 3.7\ 10^{14} W.cm^2$, $W_0 = 60\mu m$, $t_0 = 400ps$. $\lambda_0 = 1.053\mu m$.
- Initial plasma (Helium: $Z = 2$) :

$$n_0 = 0.014 n_c,\ T_{e0} = 100eV,\ T_{i0} = 30eV.$$

- Electron heat flux model:
  - Spitzer-Härm Conductivity, marginally valid for ICF : (non maxwellian electrons density functions.)
  - Brantov (98) nonlocal Conductivity. Based on a linearised theory of Fokker-Planck Valid for an "arbitrary" collisionality.
- Braginskii viscosity & ion Landau damping $-- >$ ion heat conductivity. .

Initial Density is constant in space

Brantov (non local)

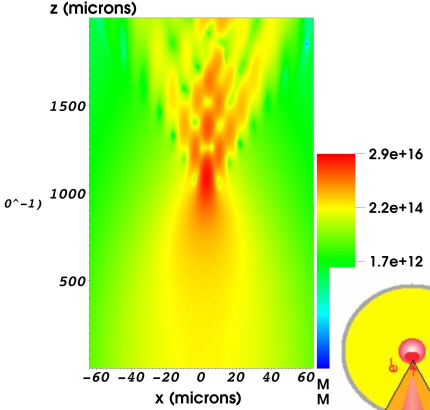

Spitzer-Härm

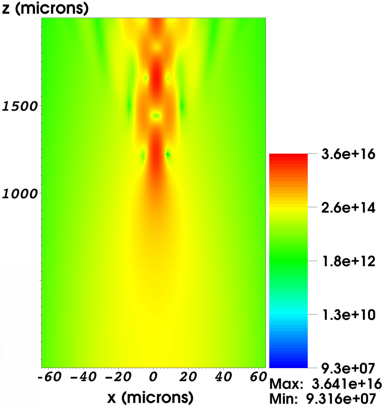

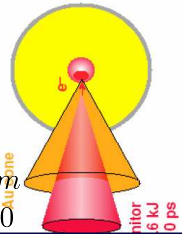

$\delta x = \delta y = 2\mu m \quad \delta z = 5\mu m$

$N_x = N_y = 256 \quad N_z = 400$

$\delta t = 5\ 10^{-2}$ps

Energy after $550ps$:$\delta x = \delta y = 2\mu m,\ \delta z = 5\mu m$

Initial Density is profiled in space

Brantov (non local)

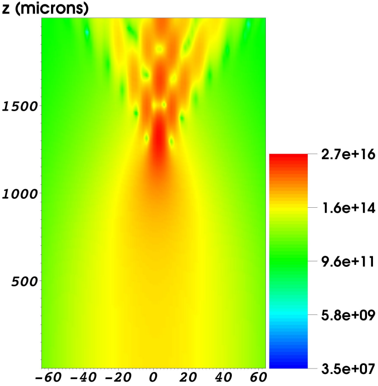

Spitzer-Härm

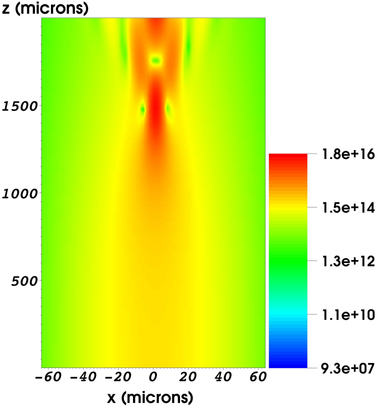

Parallel computing : Quad Itanium® II, Dual-Core, 1.6 Ghz, 128 Go

$\simeq 150 \times 10^6$variables 10^4time steps : 40H CPU with 32 cores

Tokamak plasmas : KINETIC or/and FLUID ?

- What is the range of applicability of fluids modelizations for large Tokamaks plasmas ?
- Can we accurately take into account unresolved kinetic and/or particles orbits effects on large macroscopic scaled?
- What are characteristic behaviors of “Fluid like” modelizations, their stiffness and asymptotic?
- Can we design appropriate, stable, accurate, efficient and scalable numerical approximations that are able to simulate long time MHD instabilities for ITER and DEMO?

Ballooning instability : Reduced MHD (Jorek)

Equilibrium: Flow $\simeq 40km/s$

Edge localized modes

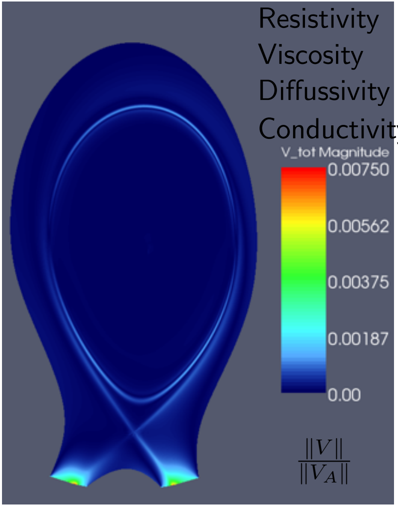

Resistivity	:	σ	$= 2\ 10^{-6}$
Viscosity	:	μ	$= 4\ 10^{-6}$
Diffussivity	:	D	$= 10^{-5}$
Conductivity	:	$\frac{\lambda_\perp}{\lambda_{//}}$	$= 10^{-6}$

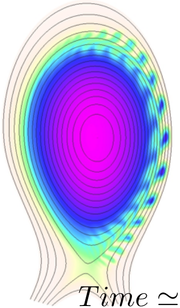

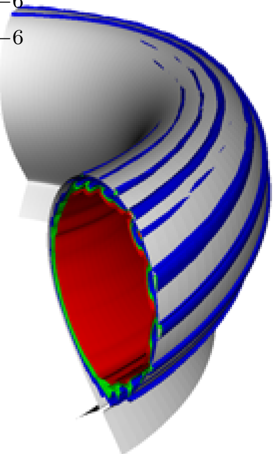

$Time \simeq 1500$ Alfvén

Temperature $\simeq 10kev$, $||V_A|| \simeq 5000km/s$,

18 Toroïdal modes used

Numerical Developments : ASTER (ANR-CIS.2006)

1. Refinable cubic-Bezier FEM (O. Czarny, G. Huysmans).
2. Direct/iterative parallel sparse matrix solver (P. Ramet, P. Henon, ...)
3. Optimized time-stepping algorithm (G. Huysmans, B. Nkonga, ...)
4. Stabilised FEM, RD schemes (R. Abgrall, R. Huart, B. Nkonga,...)
5. Extended MHD model (E. van der Plas, G. Huysmans, B. Nkonga,...)
6. Boundary conditions (M. Becoulet, G. Huysmans, ...)

ANR program Intensive Computing and Simulation (ANR-CIS.2006)
http://aster.gforge.inria.fr/index.html

Open Questions: fluid “like” models for Hot plasmas

1. Numerical schemes
   - Dynamic mesh aligned with magnetic flux surfaces.
   - High, i.e. realistic, (magnetic) Reynolds numbers
   - Resolution of boundary layers (open field line and curved boundary)
   - Long time integration: complete (internal disruption) ELM cycle (different ELM types).
2. Non-linear evolution of MHD models
   - Trigger of neoclassical transport (low collisionality, tearing modes).
   - Extended MHD (Ti-Te + Generalized Ohm’s law).
   - Interaction with micromagnetic turbulence (anomalous transport).
3. Fast particles interaction with MHD modes (nonlocal transport).
4. Charge exchange neutrals, radiation, local heating, ...